A bioinspired approach to reversibly metal binding interfaces†

Agnes C. Morrissey, [ID] ‡[a] Vishakya Jayalatharachchi,‡[a] Lukas Michalek, [ID] [a] Prasanna Egodawatta,[b] Neomy Zaquen,[c] Laura Delafresnaye [ID] *[a] and Christopher Barner-Kowollik [ID] *[a,d]

We introduce a bioinspired materials system that is capable of effectively coating surfaces, while concomitantly allowing metal ions to be reversibly bound. Specifically, we prepare a nitrogen-ligand carrying L-3,4-dihydroxyphenylalanine (L-DOPA) derivate, which can readily crosslink in aqueous systems with effective adhesion onto silicon wafers as well as stone wool fibers. Critically, the introduced system allows for reversible binding of the metal species (such as zinc cations) from aqueous solution. The reversibly binding surfaces are carefully assessed towards their metal ion binding efficiency – in contrast to non-ligand carrying coatings or uncoated surfaces – *via* surface sensitive analytical methods such as X-ray photoelectron spectroscopy, making them highly attractive candidates for applications in urban storm water filtration systems.

Introduction

Inspired by maritime organisms – especially marine mussels – molecules containing catechol units have been investigated and applied in different research fields where strong adhesion behavior to variable substrates is required.[1–3] The ability of marine mussels to withstand the dynamic ocean environment while adhering to virtually any surface has become a source of inspiration for the development of surface-based applications where the coating layer controls the material's properties. The adhesion system of marine mussels is based on mussel foot proteins and collagen proteins, which are present in the byssal thread.[4] These proteins contain different percentages of L-3,4-dihydroxyphenylalanine (L-DOPA), which is discussed as the key compound enabling the wet adhesion of the mussels.[5] Examples of applications for catechol-containing molecules feature biomedical devices,[1] biofilm prevention,[6] and bone tissue engineering.[7] Exploring the selective complexation of metal ions has become of more interest lately especially in

research fields such as wastewater treatment to remove high concentrations of metals in the environment.[8] Currently, there are two common approaches to water treatment in urban areas: natural treatments such as bioretention systems and smaller modular treatment systems like gross pollutant traps. Exploring alternative water treatment systems that can be incorporated into urban environments is critical to ensuring healthy urban waterways. Previously, the removal of heavy metals from wastewater has been based on technologies such as chemical precipitation,[9] adsorption,[10] ion exchange,[11] and electrochemical processes.[12] These conventional methods, however, have exhibited a series of shortcomings, including the generation of toxic by-products, high energy consumption, biofouling, and high cost.[13] Therefore, alternative technologies have to be explored, one option being soft matter materials with metal complexing abilities. For a potential water treatment application however, the ability of the materials system to adhere to the surface in aqueous environments while providing active treatment properties is essential. In addition to utilizing selective metal complexation for water treatment applications, in the past, metal complexation has – for example – been explored in supramolecular crosslinked self-assembled polymers.[14] The incorporation of a ligand into the L-DOPA structure presents an avenue to achieve both the adherent functionality based on the self-polymerization of L-DOPA as well as metal complexation enabled by the ligand. Specifically, the use of a tridentate chelating ligand such as ter-pyridine appears highly attractive, as it is able to coordinate heavy metal ions as shown in its application in supramolecular and coordination chemistry.[15]

*a*School of Chemistry and Physics, Queensland University of Technology (QUT), 2 George Street, 4000 Brisbane, Queensland, Australia.
E-mail: christopher.barnerkowollik@qut.edu.au, laura.delafresnaye@qut.edu.au
*b*School of Civil and Environmental Engineering, Queensland University of Technology (QUT), 2 George Street, 4000 Brisbane, Queensland, Australia
*c*Lapinus, ROCKWOOL B.V., Delfstoffenweg 2, 6045JH Roermond, The Netherlands
*d*Institute of Nanotechnology (INT), Hermann-von-Helmholtz-Platz 1, Karlsruhe Institute of Technology (KIT), 76344 Eggenstein-Leopoldshafen, Germany
†Electronic supplementary information (ESI) available. See DOI: https://doi.org/10.1039/d4lp00010b
‡These authors contributed equally to this work.
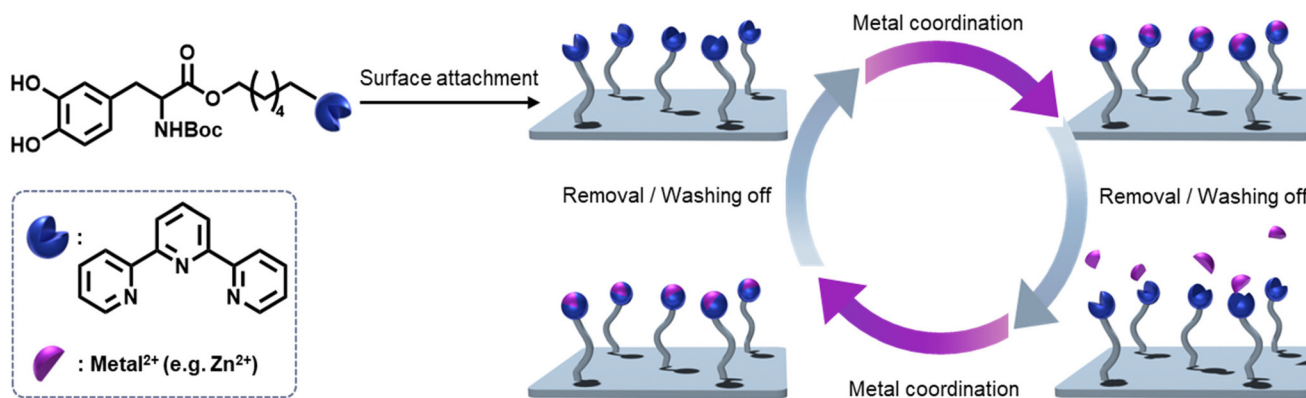
Scheme 1 General overview of the surface attachment of modified L-DOPA carrying terpyridine (compound **7**) and the reversible binding of the metal species, enabled by a terpyridine ligand and EDTA solution. The detailed synthetic route to the modified L-DOPA system is provided in Scheme 2.

Herein, we report the ability to provide strongly adhesive metal binding materials systems by introducing a terpyridine moiety into a bioinspired L-DOPA binding system to achieve an adherent coating with metal complexation properties as illustrated in Scheme 1. Moreover, we demonstrate the reversibility of the system through utilizing an ethylenediaminetetraacetic acid (EDTA) solution as a complexing agent to remove the metals on the L-DOPA coated surface. Importantly, we explore 2D and 3D fiber surfaces to investigate the applicability of the noted coating by employing surface investigation tools such as X-ray Photoelectron Spectroscopy (XPS) and Time-of-Flight Secondary Ion Mass Spectrometry (ToF-SIMS).

Results and discussion

Synthesis of bioinspired coating for structural access of 2D structures

To explore L-DOPA as a universally adherent coating for metal adsorption, we employ a systematic stepwise strategy

(Scheme 2). As noted, L-DOPA can readily self-polymerize, and our team previously reported an approach to protect and functionalize L-DOPA.[16] Specifically, the catechol and the amine functionalities are protected by employing tert-butyldimethylsilyl (TBDMS) ether and tert-butyloxycarbonyl (Boc), respectively (**2**). The carboxylic acid subsequently provides a handle to ligate various moieties, as exemplified herein with a Steglich esterification (**3**/**6**). Before surface coating, the TBDMS groups are removed via fluoride-mediated cleavage (**4**/**7**). Subsequently, the oxidative polymerization of the modified L-DOPA is performed in a Tris-HCl buffer solution as the oxidizing agent. Initially, we functionalized L-DOPA with a bromine moiety that is readily traceable via analytical techniques (e.g., XPS, ToF-SIMS) on surfaces, enabling us to investigate its surface adhesion abilities on various substrates. The Br-modified-DOPA was synthesized via the Steglich esterification of 11-bromo-1-undecanol, employing 1-ethyl-3-(3-dimethylaminopropyl) carbodiimide (EDC) as a coupling agent (**3**), proceeded by protecting the catechol and the amine functionalities with TBDMS and Boc protective groups, respectively.
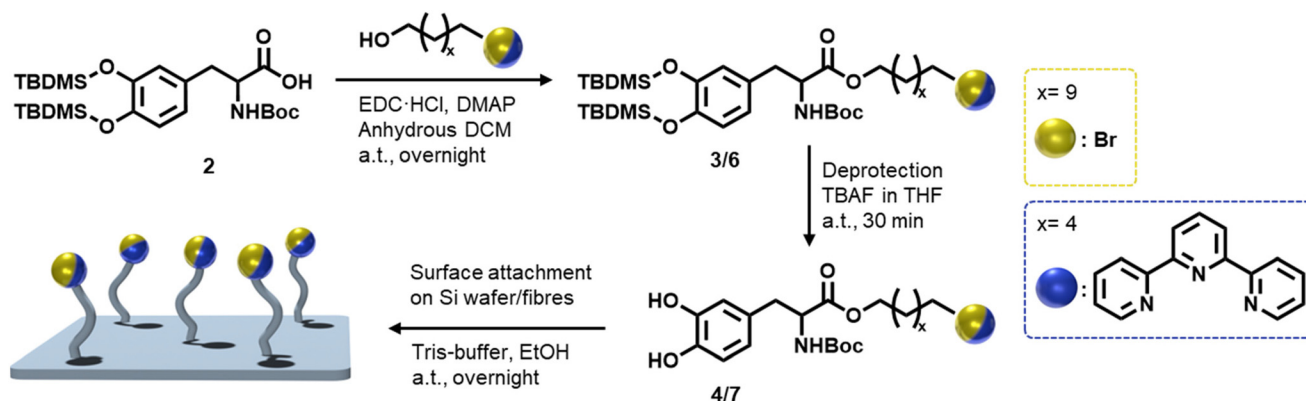

Scheme 2 Synthetic pathway to modified L-DOPA containing a bromine (yellow, compounds **3** and **4**) or terpyridine (blue, compounds **6** and **7**) moiety. Refer to the ESI† for the detailed description of the synthetic procedures (section 3) and the associated molecular characterization data (sections 4 and 5).

© 2024 The Author(s). Published by the Royal Society of Chemistry

RSC Appl. Polym., 2024, **2**, 490–496 | **491**

Subsequently, we coated silicon wafers with the Br-modified L-DOPA (**4**) due to the ease with which silicon wafers can be surface analyzed, before moving to the more complex fiber systems. Surface chemical compositions were investigated *via* XPS and ToF-SIMS. Wide scan XPS spectra unambiguously evidence the presence of Br on the Si surfaces with peaks at 181 eV and 69 eV, corresponding to Br 3p and Br 3d, respectively (Fig. 1A). XPS high resolution analysis of C 1s reveals three main components associated with C–C/C–H at 285.0 eV, C–O and C–N at 286.3 eV, O=C–O at 288.3 eV and C–Br at 289.2 eV (Fig. 1B).[17] The doublet peaks in the corresponding Br 3d high resolution spectrum (Fig. 1C) further confirm the presence of Br-modified L-DOPA (**4**) on the Si surface. In addition, we analyzed the Br-modified surfaces *via* ToF-SIMS, further confirming the surface functionalization with Br (Br isotopes peaks at 79 and 81 m/z) (Fig. S31, ESI†).[18]

Once the successful surface modification with Br-modified L-DOPA (**4**) on silicon wafers was confirmed, we examined the ability of a metal-chelating ligand carrying L-DOPA to bind metal ions once coated onto a silicon wafer. Specifically, we selected a terpyridine ligand, due to its high propensity of
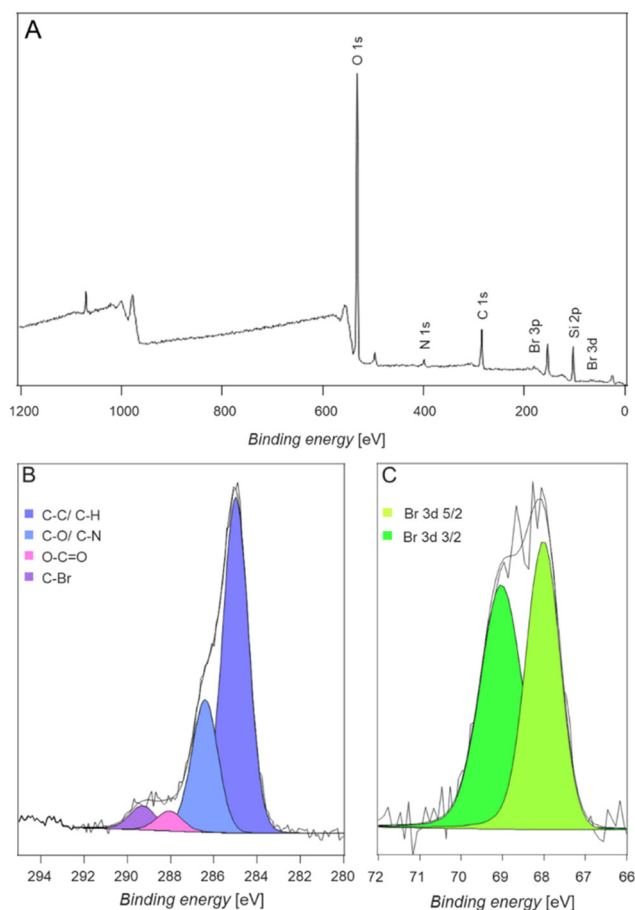
Fig. 1 (A) Wide scan XPS spectra of silicon surfaces coated with Br-modified L-DOPA. Refer to the section 7 (ESI†) for a detailed description of the surface modification procedure. Corresponding C 1s (B) and Br 3d (C) high resolution spectra.
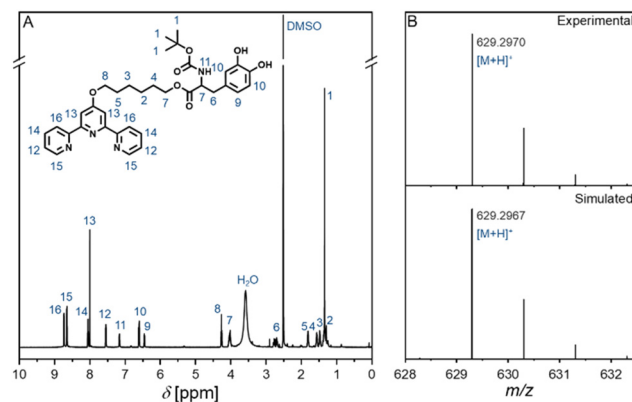
Fig. 2 (A) 600 MHz ^{1}H-NMR spectrum in DMSO-d_6 of the terpyridine carrying L-DOPA entity (**7**) (Scheme 2) as well as (B) the associated high-resolution ESI-MS spectrum. Refer to the sections 4 and 5 (ESI†) for further characterization data.

binding specific metal ions.[19] The synthesis was carried out in a similar fashion to the bromine marker synthesis, where a Steglich esterification was employed to couple the ligand onto the protected L-DOPA (Scheme 2). Fig. 2 depicts the ^{1}H-NMR spectrum and the associated electrospray ionization (ESI) mass spectrum of the terpyridine carrying L-DOPA.

In a preliminary study, we determined the ability of the binding system to coordinate metal ions *via* UV/Vis spectroscopy in solution. Specifically, the protected version (Scheme 2) of the ligand-modified L-DOPA (**7**) was dissolved in chloroform and Zn(tf)$_2$, NiCl$_2$, PbF$_2$, FeCl$_3$, and CuSO$_4$ dissolved in a chloroform/methanol (1 : 1) mixture were added (refer to the section 7 for the exact procedure and concentrations, ESI†). The obtained UV/Vis spectra (Fig. S20, ESI†) demonstrates that upon addition of a metal ion, binding to the terpyridine ligand occurs, indicated by a second absorption band arising at around 310–340 nm – depending on the metal ion – which demonstrates the successful coordination of the metal.[20]

We subsequently investigated the ligand-modified L-DOPA (**7**) system's ability to bind metal ions when coated onto Si-wafers. The Si-surface coating procedure was identical to that followed for the Br-modified L-DOPA (**4**) system (refer to the section 7, ESI†). Atomic Force Microscopy (AFM) was employed for investigating the thickness of the ligand-modified L-DOPA layer on the Si surface. To assess the film thickness, a portion of the coated surface was scratched using a scalpel. The average thickness was determined to be approximately 40.6 ± 1.1 nm (Fig. S22, ESI†). We note that the thickness exhibited non-uniformity across the surface, possibly attributed to the drying process.

The preparation of metal-ion containing solutions (Zn^{2+}, Ni^{2+}, Pb^{2+}, Fe^{3+} and Cu^{2+}) and the subsequent surface immersion procedures can be found in section 7 (ESI†). Control experiments were conducted with blank Si-wafers and Si-wafers that had been coated with non-ligand containing L-DOPA. All planar surfaces were subsequently analyzed *via* XPS and ToF-SIMS.

XPS wide scan spectra of a terpyridine functionalized and a ligand-free L-DOPA functionalized surface exposed to Zn^{2+} are depicted in Fig. 3A and B, respectively. Note that all XPS data discussed below were recorded after the surfaces had undergone identical washing procedures (refer to section 7, ESI†). The presence of Zn^{2+} is confirmed by the Zn 2p doublet peaks at 1021 eV.[21] The absence of the same peak at 1021 eV in the L-DOPA-only coated control surface suggests that the L-DOPA surface is unable to coordinate Zn^{2+} (Fig. 3B).

Similarly, XPS wide scan spectra, depicted in Fig. S24 (ESI†), demonstrate (A) the successful coordination of Cu^{2+}, indicated by the presence of Cu 2p peak at 931 eV, (B) the coordination of Ni^{2+} by the Ni 2p peak at 855 eV, (C) the coordination of Fe^{3+} by the Fe 2p peak at 710 eV, and (D) the coordination of Pb^{2+}, indicated by the presence of Pb 4d doublet peak at 413 eV. Moreover, we performed experiments with mixed metal solutions containing any of the previously mentioned metals in pairs. Interestingly, a trend in the metal binding affinity of the ligand-modified L-DOPA was observed (refer to section 11, ESI†). In summary, our results indicate that the metal coordination affinity progresses from $Fe^{3+} > Pb^{2+} > Cu^{2+} > Zn^{2+} > Ni^{2+}$. The observed trend in metal ion coordination aligns with results for metal binding in solution, and can be attributed to the different ionic radii and steric interactions.[22] After the successful proof of concept, we focused exclusively on the Zn^{2+} ions for the remainder of the study as an exemplary case.

In a subsequent critical step, we explored the ability of the ligand-modified L-DOPA (7) coated Si surfaces to remove the bound metal ions using ethylenediaminetetraacetic acid (EDTA) as an extracting ligand in free-solution. Thus, Si surfaces coated with ligand modified L-DOPA (7) coordinated with metal ions were immersed in an EDTA solution (refer to the section 7, ESI†) and subsequently analyzed by XPS. We mapped the time dependent removal of the metal ions from the surface as depicted in Fig. 4.

Since these experiments were carried out fully independently of each other, we normalized the Zn 2p atomic ratio to Si 2p atomic ratio. After a 1-minute exposure to EDTA, a sharp decrease in the Zn content on the Si surface is observed.

After 10 minutes of exposure to EDTA, all the metal was successfully removed from the Si surface. Subsequently, we explored the surface's reusability by subjecting the ligand-modified L-DOPA-coated Si surface previously exposed to EDTA for 10 minutes, to a Zn^{2+} solution. Fig. 4 demonstrates that the surface can effectively re-coordinate Zn ions following the successful removal of the metal *via* EDTA. Since the EDTA solution is basic (pH close to 10), control experiments were carried out at pH 10 (without EDTA).

XPS analyses (refer to the Fig. S28, ESI†) reveal that the metal ion is still coordinated to the ligand, therefore evidencing that the pH does not affect the removal of the metals.

3D surfaces

We subsequently moved to explore the ability of our functional coating system on 3D surfaces such as stonewool fibers. Stonewool is recognized for its ability to retain water over extended periods and gradually release it back into the environment, which has been proven by its incorporation in real world applications.[23] Focussing on enhancing this system further towards metal removal capacities will improve its applicability in active storm water treatment. Here, we assess the
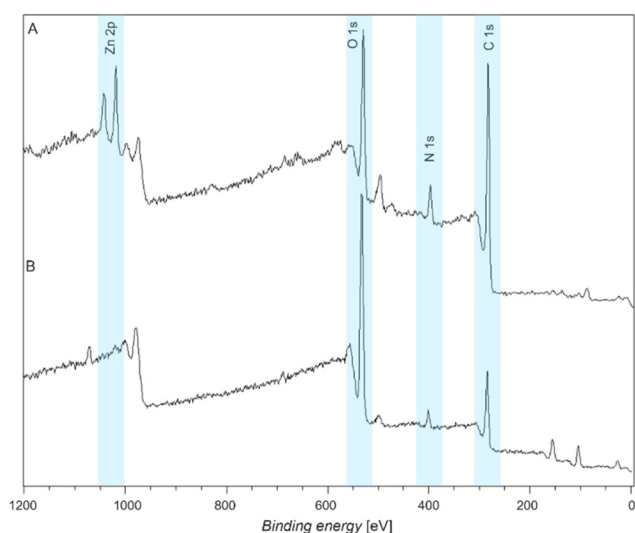
Fig. 3 (A) XPS wide scan spectra of Si-surfaces coated with ligand-modified L-DOPA, exposed to Zn^{2+}; (B) corresponding XPS wide scan spectra of Si-surfaces coated with ligand-free L-DOPA (control experiment).
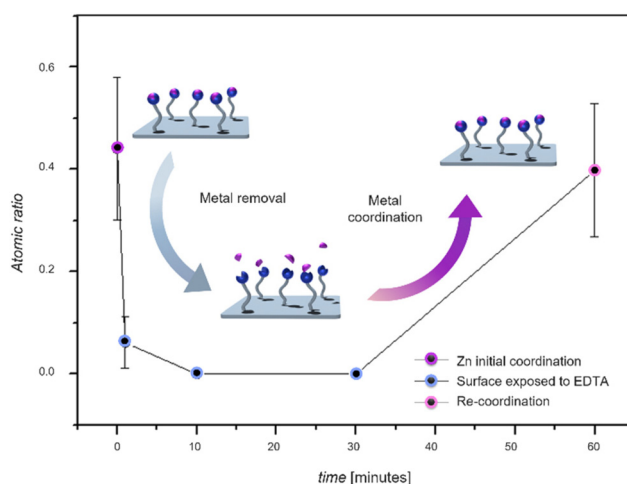
Fig. 4 Time-dependent evolution of the amount of surface bound Zn^{2+} on the surface of ligand-modified L-DOPA coated Si-wafers exposed to EDTA solution, evidencing the removal of the metal ions from the surface, and ability to re-coordinate to the ligand-modified L-DOPA, followed by XPS of the Zn 2p signal. The inset displays the time-dependent evolution of the amount of surface bound Zn^{2+} on the surface of ligand-modified L-DOPA coated Si-wafers exposed to EDTA solution, evidencing the removal of the metal ions from the surface. Error bars show ± a standard deviation by averaging 3 spots on same sample. For a detailed description of the analysis of XPS high resolution spectra and calculations, refer to section 9 of the (Fig. S26, Table S1, ESI†).

feasibility of utilizing – ultimately ligand modified L-DOPA (**7**) – to coat fibers for the purpose of removing metals salts, focusing on Zn^{2+}. The fibers were coated and subsequently exposed to metal salts in a similar fashion to the Si surfaces (refer to section 7 in the ESI†) and analyzed by both XPS and ToF-SIMS. Similarly, we initially employed the Br-modified L-DOPA (**4**) molecule to evidence that our approach is universally able to coat the fibers. Fig. 5 displays both XPS and ToF-SIMS data, evidencing the presence of the Br-modification on the fibers as indicated by the presence of a peak at 289.2 eV.[17] Further, the uniform coating was confirmed by ToF-SIMS imaging a single fiber using the Br ion signals.

The XPS wide scan spectra of fibers coated with ligand-modified L-DOPA exposed to Zn^{2+} as well as the corresponding pristine fibers exposed to Zn^{2+} are presented in Fig. 6A and B, respectively. The identification of the Zn presence is supported by the observation of doublet peaks at 1021 eV.[21] Notably, the absence of this peak at 1021 eV in the pristine fibers indicates that the pristine fibers alone do not possess the ability to coordinate with Zn^{2+} (Fig. 6B). Furthermore, Fig. 6C and D depict the ToF-SIMS images of fibers coated with ligand-modified L-DOPA coordinating Zn^{2+}, thus providing additional confirmation of the presence of Zn on the fiber surfaces. The images reveal that Zn coordination occurs uniformly across the fiber surfaces. However, variations in intensity are attributed to the non-uniform size and shape of the fibers (Fig. S21 shows the SEM image of fibers with various thickness, ESI†). A control experiment was carried out to confirm that the ligand free L-DOPA coated fibers are unable to coordinate Zn^{2+} (refer to the Fig. S27, ESI†). In addition, the fibers were exposed to metal-ion containing solutions (Ni^{2+}, Pb^{2+}, Fe^{3+} and Cu^{2+}) and XPS analyses further confirm the coordination of the metal to the ligand-modified L-DOPA coated fibers (Fig. S30, ESI†).

Moreover, to investigate the reversibility of the metal coordination on the fibers, a complexing agent – specifically EDTA –
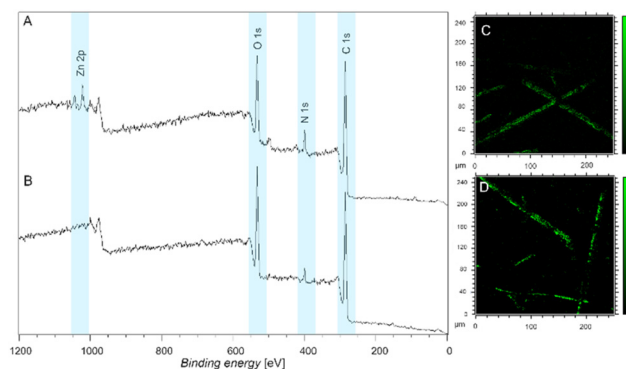

Fig. 6 (A) XPS wide scan spectra of fibers coated with ligand-modified L-DOPA (**7**), exposed to Zn^{2+} solution; (B) corresponding XPS wide scan spectra of pristine fibers exposed to Zn^{2+} solution; (C) and (D) display the ToF-SIMS spatially resolved mapping of Zn^{2+}. The images clearly demonstrate the presence of coordinated metal on the fibers. Intensity variations seen on the fibers are due to the non-uniform size of the fibers.

was utilized to remove the fiber coordinated Zn^{2+}. The wide scan XPS spectra revealed the initial coordination (Fig. 7A), as reported above, indicated with a doublet arising at 1021 eV. After immersion of the Zn^{2+} coordinated fibers in the EDTA solution for 10 minutes, the XPS spectrum (Fig. 7B) reveals the near absence of the Zn doublet at 1021 eV, thus demonstrating the successful removal of the Zn^{2+} metal ions from the fibers. The fibers were re-immersed in the Zn^{2+} solution to explore their reversibility. Fig. 7C depicts the XPS wide scan spectrum of the re-coordination experiment. The re-arising peak at 1021 eV indicates the successful re-coordination of the Zn^{2+} metal ions on the fibers, proving the reversibility of the metal ion binding, demonstrating the applicability of the coating on the 3D surfaces for the same applications as we have shown for the Si wafers (2D surfaces).
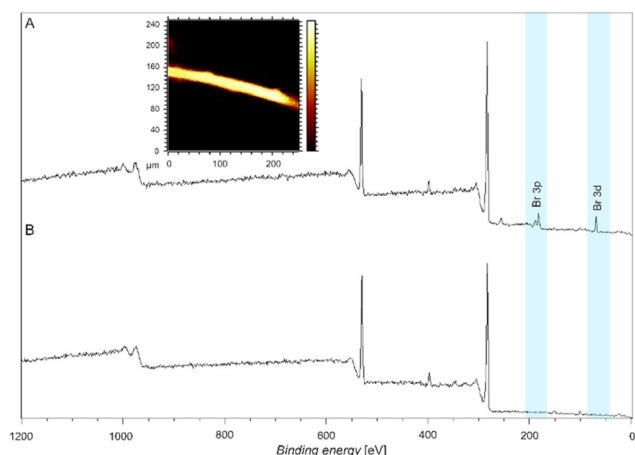
Fig. 5 Wide scan XPS spectra of (A) a fiber coated with Br-modified L-DOPA (refer to the section 7 (ESI†) for a detailed description of the surface modification procedure) and inset showing the ToF-SIMS image of a single fiber. The yellow colour represents the Br-fragment. (B) XPS spectrum of a pristine fiber.
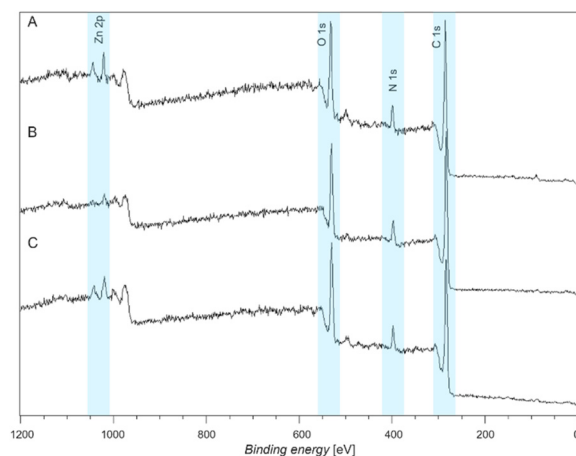
Fig. 7 XPS spectra of (A) Zn^{2+} coordinated to ligand-modified L-DOPA coated fibers, (B) Zn^{2+} coordinated fibers exposed to EDTA for 10 min, and (C) re-coordination of Zn^{2+} to the ligand-modified L-DOPA coated fibers, after exposing to EDTA for 10 minutes.

Conclusions

Metal ions are a major contributor of wastewater pollutants, and the selective complexing of metal ions for wastewater treatment is one of the most promising routes to water treatment. We introduce a bioinspired material capable of efficiently coating surfaces, while concomitantly allowing metal ions (*e.g.*, Zn^{2+}, Cu^{2+}, Pb^{2+}, Fe^{3+}, and Ni^{2+}) to be reversibly bonded, as exemplified with Zn^{2+}. Specifically, we prepared L-DOPA derivates which can readily crosslink in aqueous systems with effective adhesion onto silicon wafers as well as stone wool fibers. Critically, the L-DOPA can be functionalized with markers (*e.g.*, bromine) to assist on-surface characterization or a ligand (*e.g.*, terpyridine) able to capture metal ions. The coated surfaces were carefully assessed towards their metal ion binding efficiency – in contrast to non-ligand carrying coatings or uncoated surfaces – *via* surface sensitive analytical methods including Time of Flight Secondary Ion Mass Spectrometry and X-ray Photoelectron Spectroscopy. Furthermore, we investigated the reversibility of the binding for material recovery using a chelating agent (*i.e.*, EDTA). XPS analyses confirmed the removal of metal ions from the surfaces, with the ability to recapture them. Demonstrated on both 2D flat surfaces (*i.e.*, silicon wafers) and 3D textured stone wool fibers, this bioinspired coating approach holds great promise as a universal metal-binding surface coating. In addition, the simplicity of the coating procedure may readily be translated into a flow coating process, enabling the efficient coverage of large areas. The versatility and effectiveness of our approach, combined with its ability for reversible metal binding, make our coating highly attractive candidates for real world applications, such as the removal of pollutants from water.

Author contributions

L. M., P. E., L. D. and C. B.-K. conceptualized and supervised the project. A. C. M. and V. J. performed the experiments, analyzed the data, and wrote the manuscript. L. M., P. E., N. Z., L. D. and C. B.-K. revised and edited the manuscript.

Conflicts of interest

The authors have filed a priority patent application protecting the herein described technology.

Acknowledgements

References

1 J. Song, T. M. Lutz, N. Lang and O. Lieleg, *Adv. Healthcare Mater.*, 2021, **10**, 2000831.

2 K. Jiang, F. Li, X. Zhao and Y. Pan, *ACS Appl. Nano Mater.*, 2022, **5**, 8038–8047.

3 Y. Chen, K. Ai, J. Liu, X. Ren, C. Jiang and L. Lu, *Biomaterials*, 2016, **77**, 198–206.

4 H. Lee, S. M. Dellatore, W. M. Miller and P. B. Messersmith, *Science*, 2007, **318**, 426–430.

5 J. H. Waite, *Integr. Comp. Biol.*, 2002, **42**, 1172–1180.

6 H. Woehlk, M. J. Trimble, S. C. Mansour, D. Pletzer, V. Trouillet, A. Welle, L. Barner, R. E. W. Hancock, C. Barner-Kowollik and K. E. Fairfull-Smith, *Polym. Chem.*, 2019, **10**, 4252–4258.

7 W.-B. Tsai, W.-T. Chen, H.-W. Chien, W.-H. Kuo and M.-J. Wang, *J. Biomater. Appl.*, 2014, **28**, 837–848.

8 O. A. Oyetade, V. O. Nyamori, B. S. Martincigh and S. B. Jonnalagadda, *RSC Adv.*, 2016, **6**, 2731–2745.

9 A. Azimi, A. Azari, M. Rezakazemi and M. Ansarpour, *ChemBioEng Rev.*, 2017, **4**, 37–59.

10 W. S. Chai, J. Y. Cheun, P. S. Kumar, M. Mubashir, Z. Majeed, F. Banat, S.-H. Ho and P. L. Show, *J. Cleaner Prod.*, 2021, **296**, 126589.

11 J. Wu, T. Wang, J. Wang, Y. Zhang and W.-P. Pan, *Sci. Total Environ.*, 2021, **754**, 142150.

12 L. Yang, W. Hu, Z. Chang, T. Liu, D. Fang, P. Shao, H. Shi and X. Luo, *Environ. Int.*, 2021, **152**, 106512.

13 R. Shrestha, S. Ban, S. Devkota, S. Sharma, R. Joshi, A. P. Tiwari, H. Y. Kim and M. K. Joshi, *J. Environ. Chem. Eng.*, 2021, **9**, 105688.

14 D. Liu, M. Chen, K. Li, Z. Li, J. Huang, J. Wang, Z. Jiang, Z. Zhang, T. Xie, G. R. Newkome and P. Wang, *J. Am. Chem. Soc.*, 2020, **142**, 7987–7994.

15 A. Wild, A. Winter, F. Schlütter and U. S. Schubert, *Chem. Soc. Rev.*, 2011, **40**, 1459–1511.

16 C. M. Preuss, T. Tischer, C. Rodriguez-Emmenegger, M. M. Zieger, M. Bruns, A. S. Goldmann and C. Barner-Kowollik, *J. Mater. Chem. B*, 2014, **2**, 36–40.

17 Y. Zhan, X. Wan, S. He, Q. Yang and Y. He, *Chem. Eng. J.*, 2018, **333**, 132–145.

18 O. Altintas, M. Glassner, C. Rodriguez-Emmenegger, A. Welle, V. Trouillet and C. Barner-Kowollik, *Angew. Chem., Int. Ed.*, 2015, **54**, 5777–5783.

19 S. Bode, L. Zedler, F. H. Schacher, B. Dietzek, M. Schmitt, J. Popp, M. D. Hager and U. S. Schubert, *Adv. Mater.*, 2013, **25**, 1634–1638.

© 2024 The Author(s). Published by the Royal Society of Chemistry

RSC Appl. Polym., 2024, **2**, 490–496 | **495**

20 Y. Zhang, P. Zhou, B. Liang, L. Huang, Y. Zhou and Z. Ma, *J. Mol. Struct.*, 2017, **1146**, 504–511.

21 C. K. Rojas-Mayorga, D. I. Mendoza-Castillo, A. Bonilla-Petriciolet and J. Silvestre-Albero, *Adsorpt. Sci. Technol.*, 2016, **34**, 368–387.

22 H. A. Saadeh, E. A. A. Shairah, N. Charef and M. S. Mubarak, *J. Appl. Polym. Sci.*, 2012, **124**, 2717–2724.

23 S. Bougoul, S. Ruy, F. de Groot and T. Boulard, *Sci. Hortic.*, 2005, **104**, 391–405.